The Topology of Mutated Driver Pathways

Raouf Dridi[*1], Hedayat Alghassi[†1], Maen Obeidat[‡2], and Sridhar Tayur[§1]

[1]Quantum Computing Group, Tepper School of Business, Carnegie Mellon University, Pittsburgh, PA
[2]The University of British Columbia Center for Heart Lung Innovation, St Paul's Hospital Vancouver, Vancouver, BC

December 3, 2019

Abstract

Much progress has been made, and continues to be made, towards identifying candidate mutated driver pathways in cancer. However, no systematic approach to understanding how candidate pathways relate to each other for a given cancer (such as Acute myeloid leukemia), and how one type of cancer may be similar or different from another with regard to their respective pathways (Acute myeloid leukemia vs. Glioblastoma multiforme for instance), has emerged thus far. Our work attempts to contribute to the understanding of *space of pathways* through a novel topological framework. We illustrate our approach, using mutation data (obtained from TCGA) of two types of tumors: Acute myeloid leukemia (AML) and Glioblastoma multiforme (GBM). We find that the space of pathways for AML is homotopy equivalent to a sphere, while that of GBM is equivalent to a genus-2 surface. We hope to trigger new types of questions (i.e., allow for novel kinds of hypotheses) towards a more comprehensive grasp of cancer.

[*]rdridi@andrew.cmu.edu
[†]halghassi@cmu.edu
[‡]Maen.Obeidat@hli.ubc.ca
[§]stayur@cmu.edu

1

Key words: Cancer genomics, mutation data, acute myeloid leukemia, glioblastoma multiforme, persistent homology, simplicial complex, topological data analysis, Betti numbers, algebraic topology.

1 Introduction

Let us begin by recalling a quote of Henri Poincare:

> Science is built up of facts, as a house is built of stones; but an accumulation of facts is no more a science than a heap of stones is a house.

Cancer is driven by somatic mutations that target signaling and regulatory pathways that control cellular proliferation and cell death [25]. Understanding how this happens is of paramount importance in order to improve our ability to intervene and attack cancer. Since the advent of DNA sequencing technologies, our understanding has progressed enormously and resulted in useful therapies.[1]

Notwithstanding the above, cancer morbidity is still very high and our understanding is still incomplete. Certainly, finding more relevant pathways will be helpful. Indeed we have developed novel formulations and algorithms that are computationally effective in doing so, a subject of our companion paper ([1] that builds on our work [2, 3]). We also believe that to start building a house it is not enough to simply accumulate more stones faster. To that end,

---

[1] Current advances include the introduction of a single anti-cancer agents, which simply bind with growth factor receptors stopping abnormal cell proliferations. For instance, in the context of breast cancer, Herceptin antibody stops cells abnormal proliferation signals by binding with the excess of growth factor receptors on the cell surface caused by point mutations in the gene Her2. Gleevec is a second example. It is used to treat chronic myeloid leukemia, which is a type of blood cell tumor due to an inappropriate gene fusion product of a translocation in chromosomes 9 and 22. The resulting fusion gene BCR-ABL has an increased kinase activity, resulting in an increase in proliferation signals. Similar to Herceptin, Gleevec blocks the growth signals that the abnormal fusion gene generates and thus prevents the cell proliferation. More sophisticated approaches include immunotherapy that activates the immune system against cancer cells as well as the use of combinations of therapeutic agents to attack multiple pathways fundamental in cancer development, preventing resistance from occurring.

in this paper, we look at whether the stones that we have identified so far form patterns that can help us build a house, using methods from algebraic topology (see Table 1).

The view we are taking here is also articulated in *The Hallmarks of Cancer* ([7]):

> Two decades from now, having fully charted the wiring diagrams of every cellular signaling pathway, it will be possible to lay out the complete "integrated circuit of the cell" upon its current outline (Figure 1). We will then be able to apply the tools of mathematical modeling to explain how specific genetic lesions serve to reprogram this integrated circuit... One day, we imagine that cancer biology and treatment–at present, a patchwork quilt of cell biology, genetics, histopathology, biochemistry, immunology, and pharmacology–will become a science with a conceptual structure and logical coherence that rivals that of chemistry or physics.

Pathways	Algebraic topology
Regulatory/signaling pathway	simplex
The Emergent integrated circuit of the cell	simplicial complex K_ε
Number of patients shared between two genes	persistent parameter ε

Table 1: Correspondence between pathways and algebraic topology.

Our topological journey departs from the (well trodden) path that recognized that signaling or regulatory pathways can be viewed as *independent sets* (modulo some notion of tolerance) in a matrix with rows as patients and columns as genes, which is used in determining new pathways via different computational methods (see our companion paper [1] and previous works [21, 22, 5, 18, 10]). Our key insight is that these pathways (however discovered), when grouped together, define a *simplicial complex* which is, pictorially, a polytope with faces given by those pathways. This vantage point connects us to the marvellous world of topology where simplicial complexes are the prototypes of spaces with shapes. Our journey explores this *notion of shape* in cancer genomics.

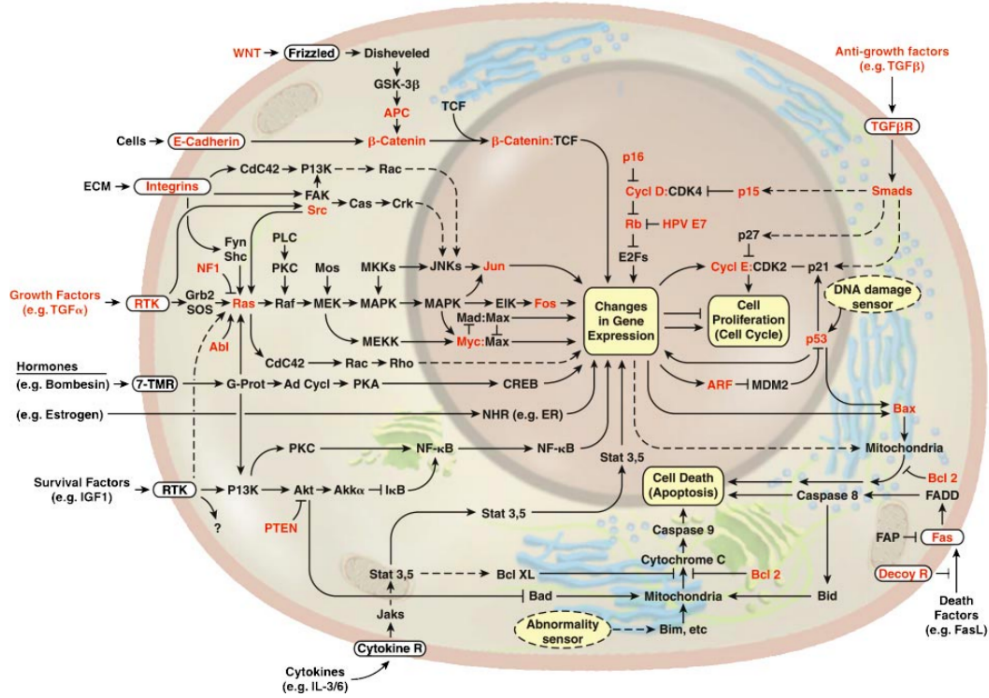Our framework is built on this sequence of assignments:

Figure 1: Cell circuitry, wiring pathways, resembles electronic integrated circuits. A full understanding of this picture will, one day, replace the present day patchwork with a more rational approach based on conceptual structures and logical coherence similar to those encountered in chemistry and physics [7].

$$\textbf{MutationData} \quad \rightarrow \quad \textbf{graphs} \quad \rightarrow \quad \textbf{SpaceOfPathways} \quad \rightarrow \quad \textbf{ShapeMeasurements}$$
$$X \qquad\qquad \mapsto \qquad G \qquad \mapsto \qquad \mathcal{N}(K) \qquad\qquad \mapsto \qquad H_*(\mathcal{N}(K))$$

where:

- G is the mutation graph. That is, is the graph defined by the set of genes in X where two genes are connected if they have harboured mutations for the same patients. K is the simplicial complex given by the set of all independent sets of G. The underlying mathematics detailed in [6] is based on the so-called Mayer-Vietoris construction, which itself is articulated around clique covering the graph G. We

4

prove in [6] that, for a large class of graphs, such coverings provide most of the simplices of K.

- $\mathcal{N}(K)$ is the space of pathways. The facets (maximal independent sets) of K are the pathways, and their nerve defines the space of pathways $\mathcal{N}(K)$. Pictorially, the space of pathways is visualized through its 1-skeleton of the graph with pathways as vertices and where two pathways are connected by an edge if they intersect.

- $H_*(\mathcal{N}(K))$ is the homology of the space of pathways, that is, the shape measurements of the space of pathways.

We have applied our approach to two different mutation data obtained from TCGA: Acute myeloid leukemia (AML) [14] and Glioblastoma multiforme (GBM) [13]. For both the data, we have computed the assignment

$$\text{tumor} \to \text{space of pathways} \tag{1.1}$$

using persistent homology.[2] Our calculation shows that the space of pathways for AML mutation data is homotopy equivalent to a sphere, while in the case of GBM data, the space of pathways is homotopy equivalent to figure eight (genus-2 surface).

2 Related works

The motivation for the present work originates from the work of the Raphael Lab, centred around the Dendrix algorithm [23], and its later improvements including CoMEt [9]. Both algorithms are in widespread use in whole-genome analysis–for instance, in [16, 17, 4, 20]. Building on those foundations, our work extends in the following two directions: First, the two key notions of exclusivity and coverage are abstracted here by the two simplicial complexes K_ε and K_η or, more precisely, by the filtrations of simplicial complexes $K_{\varepsilon_0} \subset \cdots \subset K_{\varepsilon_\ell}$ and $K_{\eta_0} \subset \cdots \subset K_{\eta_{\ell'}}$, where we allow the two parameters to vary: $\varepsilon_0 \le \varepsilon \le \varepsilon_\ell$ and $\eta_0 \le \eta \le \eta_{\ell'}$. We do so because, in reality, the assumptions

---

[2]In the language of *Homotopy Type Theory (HoTT)* [19], this procedure translates into: $tumor \mapsto (\infty, 1)-category$. This $(\infty, 1)-$category is an $(\infty, 1)-$topos (a logical structure) in the sense of Lurie [12], so it obeys the *axioms* of HoTT.

that driver pathways exhibit both high coverage and high exclusivity need not to be strictly satisfied. The functoriality of persistent homology, which takes the two filterations as input, handles this elegantly; we decide on the values of these two parameters after computing the barcodes. This type of analysis is not present in the aforementioned works. Second, motivated by the *naturality* of the constructions, the present paper goes beyond the computational aspects and ventures into the *conceptuality of cancer*. We have introduced the notion of the topological space of pathways $\mathcal{N}$, together with its homology spaces, as a paradigm to rationalize the extraordinary complexity of cancer. To the best of our knowledge, this is a "provocative" idea that has not been explored before.

Another related set of works is [11] and [15] (from Stanford's applied topology group), which also use algebraic topology tools in cancer. However, they differ from ours on two counts: the nature of the problem treated and the methodology used. The algorithm introduced, called Mapper, is a topological clustering algorithm, and it is not based on persistent homology. Mapper was used to identify a subgroup of breast cancers with excellent survival, solely based on topological properties of the data.[3]

3 Connecting to algebraic topology

Different errors occurring during data preparation (i.e., sequencing step, etc.) affect the robustness of the results. This implies that the computed pathways are likely to be affected by these errors and can not be considered as a robust finding without explicitly modeling the error in our constructions. To that end, the assignment we mentioned above is done as follows:

1. We think about the number of patients that are shared between two genes as a parameter ε (thus, absolute exclusivity corresponds to taking this parameter to zero).

2. Instead of applying our procedure once, we apply it for a range of values of the exclusivity parameter ε. That is, we consider a filtration of graphs (instead of one):

---

[3]Commercial applications of this approach in various different areas of practice are tackled through Ayasdi.

$$G_{\varepsilon_0} \subset \cdots \subset G_{\varepsilon_\ell} \tag{3.1}$$

where for each graph G_ε two genes are connected if they have harboured mutations concurrently for at least ε patients. This yields a second filtration of simplicial complexes (we call such a filtration, a *persistent pathway complex*)

$$K_{\varepsilon_0} \subset \cdots \subset K_{\varepsilon_\ell} \tag{3.2}$$

where K_ε is one of the three complexes we define below.

3. Measure the shape (the homology) of the different pathway spaces and then "average" the shape measurements that are obtained.

This (practical) version of homology is what we refer to as persistent homology. It tracks the persistent topological features through a range of values of the parameter; genuine topological properties persist through the change of the parameter whilst noisy observations do not (all of these will be made precise below). The key point is that the mapping $G_\varepsilon \mapsto K_\varepsilon$ is *functorial*; that is, it sends a whole filtration (i.e., 3.1) into another filtration (i.e., 3.2). In other words, it is not only sending graphs to simplicial complexes but it is also preserving their relations. This functoriality is at the heart of persistent homology.

3.1 The Gene-Patient graph

Consider a mutation data for m tumors (i.e., patients), where each of the n genes is tested for a somatic mutation in each patient. To this data we associate a mutation matrix B with m rows and n columns, where each row represents a patient and each column represents a gene. The entry B_{ig} in row i and column g is equal to 1 if patient i harbours a mutation in gene g and it is 0 otherwise. For a gene g, we define the fiber

$$\mathsf{Patients}(g) = \text{the set of patients in which } g \text{ has mutated.} \tag{3.3}$$

Definition 1 *The* mutation graph *associated to B and $\varepsilon > 0$ is the graph G_ε whose vertex set is the set of genes and whose edges are pairs of genes (g, g') such that*

$$|\mathsf{Patients}(g) \cap \mathsf{Patients}(g')| \geq \varepsilon. \tag{3.4}$$

There are evidences that pathways can be treated as independent sets of mutation graphs (although not stated graph-theoretically) [24, 26].

3.2   The space of pathways

We would like to assign to the mutation graph an independence complex. We present below two different functorial ways to do so.

Definition 2 *Given a mutation graph G_ε, its* persistent pathway complex K_ε *is the independence complex of G_ε (or equivalently, the clique complex of $\overline{G}_\varepsilon$, the complement of G_ε).*

We also define the persistent pathway complex K_η.

Definition 3 *The persistent pathway complex K_η is defined as follows. Fix $\varepsilon = \varepsilon_0$ and let $G = G_{\varepsilon_0}$. The complex K_η is the complex generated by all independent sets S of G with coverage*

$$\sum_{g \in S} \mathsf{Patients}(g) \geq \eta \tag{3.5}$$

where the counting $g \in S$ is done without redundancy.

The following definition is also valid for the persistent pathway complex K_η.

Definition 4 *The space of pathways of a persistent pathway complex K_ε is the nerve generated by the facets of the complex, that is, the simplicial complex where $\{i_0, \cdots, i_\ell\}$ is a simplex if and only if the facets indexed with $i_0, \cdots, i_\ell$ have a non empty intersection. We denote the space of pathways by $\mathcal{N}_\varepsilon$.*

The space of pathways is visualized through its 1-skeleton: the graph with pathways as vertices, and two pathways are connected if they intersect (see Figures 3 and 4).

3.3   A primer on persistent homology

Recall that our plan is to compute the persistent homology of the independence complex K_ε. We have explained that this is simply computing the homology of K_ε for a range of increasing values of the parameter ε. In this

section, we explain this notion of homology (which we have introduced as measurements of the shape of the space K_ε). For simplicity, we drop out the subscript ε from the complex K_ε. It is also more convenient to introduce homology for clique complexes (for independence complexes, it suffices to replace, everywhere below, cliques with independent sets).

The homology of the simplicial complex K (now a clique complex of G) is a sequence of $\mathbb{Z}$-vector spaces (i.e., vector spaces with integer coefficients):

$$H_*(K) := H_0(K), \quad H_1(K), \quad H_2(K), \quad \ldots \tag{3.6}$$

defined as follows:

- The zeroth vector space $H_0(K)$ is spanned by all connected components of K; thus, the dimension $\beta_0 := \dim(H_0(K))$ gives the number of connected components of the space.

- The first homology space $H_1(K)$ is spanned by all closed chains of edges (cycles) in G which are not triangles – see Figure 2; in this case, the dimension $\beta_1 := \dim(H_1(K))$ gives the number of "holes" in the space.

- Similarly, the second space $H_2(K)$ is spanned by all 2-dimensional enclosed three dimensional "voids" that are not tetrahedra (as in Figure 3 below).

Higher dimensional spaces are defined in a similar way (although less visual). Their dimensions count non trivial high dimensional voids. The dimensions $\beta_i := \dim(H_i(K))$ are called Betti numbers and provide the formal description of the concept of shape measurements.[4]

We move now to the notion of persistent homology and make it a bit more precise. For that, let us reintroduce the persistent parameter ε and let K_ε be again an independence complex. It is clear that if $|\mathsf{Patients}(g) \cap \mathsf{Patients}(g')| \geq \varepsilon_1$ and $\varepsilon_1 \geq \varepsilon_2$ then the pair (g, g'), which is an edge in G_{ε_1}, is also is an edge in G_{ε_2}. This means that G_{ε_1} is a subgraph of G_{ε_2}; thus, we have $K_{\varepsilon_2} \subset K_{\varepsilon_1}$

---

[4]In textbooks, one typically starts with a continuous space (for instance, a doughnut shaped surface) and then triangulizes it, yielding the simplicial complex K. The homology of the continuous space is the homology of its discretization K that we introduced pictorially above. Appendix A, on page 20, explains how to compute homology using quantum computers or QUBO-solvers such as [2].
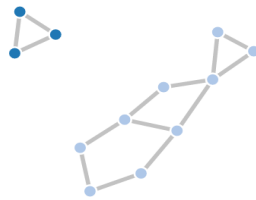
Figure 2: The graph has two connected components, which implies $\beta_0 = 2$. It also has two cycles that are not triangles; thus, $\beta_1 = 2$. Higher Betti numbers are zero.
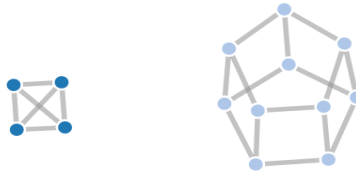

Figure 3: The graph has two connected components, giving $\beta_0 = 2$. It also has 7 cycles that are not triangles, which yields $\beta_1 = 7$. Higher Betti numbers are zero here as well. Now, if the different sides of the hexagonal prism (right component) are covered with triangles, then we get instead $\beta_1 = 0$ and $\beta_2 = 1$.

whenever $\varepsilon_1 \geq \varepsilon_2$ (since an independent set for a given graph is also an independent set for any of its subgraphs). The mapping $\varepsilon \mapsto K_\varepsilon$ is functorial. It turns out that homology itself is functorial and all this functoriality is the mathematical reason that the following is correct: one can track the Betti numbers over a range of values $\varepsilon_1 \geq \varepsilon_2 \geq \varepsilon_3 \geq \cdots$ and consider the subrange where the Betti numbers are not changing (significantly). Pathways within this subrange are considered to have passed our test and declared robust computations.

4   Real mutation data

We have applied our approach to two mutation data (formulations and algorithms are available in [1]): Acute myeloid leukemia [14] and Glioblastoma multiforme [13]. For both data, we have computed the assignment *tumor* $\mapsto$ *pathways* through persistent pathway complexes (thus, declared robust output). The complete result is presented in long tables given in the Appendix. Interestingly, our calculation also shows that AML data is homotopy equivalent to a sphere while GBM data is homotopy equivalent to figure eight (genus-2 surface).

4.1   Acute myeloid leukemia data

The data has a cohort of 200 patients and 33 genes ([14]). We have chosen the coverage threshold $\eta = 80$ patient. We also neglected all genes that have fewer than 6 patients. These numbers are chosen based on the stability of barecodes for pairs $(\varepsilon, \eta) \geq (6, 80)$, while barecodes for pairs less than $(6, 80)$ exhibit strong variations. This is also consistent with the fact that choosing genes with fewer than 5 or 6 patients is not common in such studies (genes with low numbers of patients are not considered robust enough, and are very prone to errors. This extra precaution is commonly used in the field). Now for the numbers of patients and coverage we have chosen, the Betti numbers are computed for various values of ε in the table below:

ε	$|\mathcal{N}_\varepsilon|$	$density(\mathcal{N}_\varepsilon)$	β_i
1	6	0.86	$1, 0, 0, \cdots$
2	84	0.97	$1, 0, 0, \cdots$
3	50	1	$1, 0, 0, \cdots$

Figure 4 below gives the 1-skeleton of the nerve $\mathcal{N}_\varepsilon := \mathcal{N}(K_\varepsilon)$ for $\varepsilon = 1$. The Betti numbers β_i are not changing; thus, $\varepsilon = 1$ is a reasonable choice. Recall that each node represents a pathway and two pathways are connected if they intersect (as sets of genes). We have used different colors to represent different pathways as described in the table below (no other meaning for the coloring).

Figure 4: The 1-skeleton of the nerve $\mathcal{N}_\varepsilon$ for $\varepsilon = 1$ for AML data. In this case, the nerve is homotopy equivalent to the sphere. The different pathways represented by the nodes are given in the table above.

Color	Genes in the pathway
Blue	'PML.RARA', 'MYH11.CBFB', 'RUNX1.RUNX1T1', 'TP53', 'NPM1', 'RUNX1'
Blue light	'PML.RARA', 'MYH11.CBFB', 'RUNX1.RUNX1T1', 'TP53', 'NPM1', 'MLL.PTD'
Orange	'PML.RARA', 'MYH11.CBFB', 'RUNX1.RUNX1T1', 'DNMT3A'
Orange light	'Other Tyr kinases', 'MYH11.CBFB', 'MLL.PTD', 'NPM1'
Green	'MLL-X fusions', 'TP53', 'FLT3'
Green light	'Other Tyr kinases', 'MYH11.CBFB', 'DNMT3A', 'MLL-X fusions'

4.2   Glioblastoma multiforme data

The second mutation data is taken from [13]. It has 84 patients and around
100 genes. Approximately, 70% of the genes have very low coverage so we
removed them from the data; precisely, we have removed all genes with fewer
than 10 patients. We have used the complex K_η, with ε fixed to 7 because
lower values don't exhibit stable topologies; that is, barcodes are essentially
one point long. This is a different choice of complex from the complex K_ε
that we used with the previous AML data, which interestingly doesn't yield
noticeable stability–a possible explanation of this is the small size of the data
(i.e., number of patients). Recall that the definitions of the two complexes
are given on page 8 (definitions 2 and 3). In the table below, one can see that
the topology stabilizes for the first three values of η. Any choice of pathways
within this range is considered robust (proportionate to the small size of the
data).

η	$|\mathcal{N}_\eta|$	$density(\mathcal{N}_\eta)$	β_i
66	15	0.73	$1, 2, 0, \cdots$
67	14	0.74	$1, 2, 0, \cdots$
68	12	0.72	$1, 2, 0, \cdots$
69	6	0.6	$1, 0, 0, \cdots$
70	50	1	$1, 0, 0, \cdots$

Figure 5: The nerve for the space of pathways for GBM data (see table below for the legend). The barcodes are stable in the first part of the table, which indicates that the nerve is homotopy equivalent to a genus-2 surface.

The following table provides the legend for the Figure 5 corresponding to the GBM data:

Color	Genes in the pathway
blue	RB1, NF1, CYP27B1, CDKN2B
blue light	RB1, NF1, MDM2, AVIL-CTDSP2, CDKN2B
orange	TP53, MDM2, OS9, CDKN2A
orange light	TP53, MDM2, AVIL-CTDSP2, CDKN2A
green	TP53, MDM2, DTX3, CDKN2A
green light	RB1, NF1, CDK4, CDKN2B
brown	TP53, CDK4, CDKN2A
brown light	TP53, CYP27B1, CDKN2A
purple	TP53, MDM2, AVIL-CTDSP2, MTAP
purple light	TP53, MDM2, DTX3, MTAP
red	RB1, NF1, MDM2, OS9, CDKN2B
pink	TP53, MDM2, OS9, MTAP

5 Conclusion

The main goal of this paper was to suggest a study of the *space of cancer pathways*, using the natural language of algebraic topology. We hope that the consideration of the pathways collectively, that is, as a topological space, helps to reveal novel relations between these pathways. Indeed, we have seen that the homology in the case of AML indicates that the mutation data has the shape of a sphere.[5] However, in the case of GBM, the final set of pathways has the topology of a double torus (or, more technically, a genus-2 surface). This intriguing observation raises the question of whether these facts translate into a new biological understanding about cancer. Studying the space of pathways of other cancers will be illuminating as well, if they

---

[5]Using a different visual representation, Vogelstein found AML to be very different from other cancers. Indeed, that has allowed many scientists to speculate that such genetically simple tumors are more susceptible to drugs, and thus intrinsically more curable.

also show similar structures, and we can classify cancers by the topology of their mutated driver pathways. This is an example of the new type of hypotheses one can now formulate about the data. Eventually, our goal (recalling Poincare) is to help build a house by revealing patterns among the stones. Let us close with a quote from *The Emperor of All Maladies* (page 458):

> The third,[6] and arguably most complex, new direction for cancer medicine is to integrate our understanding of aberrant genes and pathways to explain the *behavior* of cancer as a whole, thereby renewing the cycle of knowledge, discovery and therapeutic intervention.

References

[1] H. Alghassi, R. Dridi, A. G. Robertson, and S. Tayur. Quantum and Quantum-inspired Methods for de novo Discovery of Altered Cancer Pathways. *bioRxiv:10.1101/845719*, Nov. 2019.

[2] H. Alghassi, R. Dridi, and S. Tayur. GAMA: A Novel Algorithm for Non-Convex Integer Programs. *arXiv:1907.10930*, July 2019.

[3] H. Alghassi, R. Dridi, and S. Tayur. Graver Bases via Quantum Annealing with Application to Non-Linear Integer Programs. *arXiv:1902.04215*, Feb. 2019.

[4] F. Bertucci, C. K. Y. Ng, A. Patsouris, N. Droin, S. Piscuoglio, N. Carbuccia, J. C. Soria, A. T. Dien, Y. Adnani, M. Kamal, S. Garnier, G. Meurice, M. Jimenez, S. Dogan, B. Verret, M. Chaffanet, T. Bachelot, M. Campone, C. Lefeuvre, H. Bonnefoi, F. Dalenc, A. Jacquet, M. R. De Filippo, N. Babbar, D. Birnbaum, T. Filleron, C. Le Tourneau, and F. André. Genomic characterization of metastatic breast cancers. *Nature*, 569(7757):560–564, 2019.

[5] G. Ciriello, E. Cerami, C. Sander, and N. Schultz. Mutual exclusivity analysis identifies oncogenic network modules. *Genome Res*, 22(2):398–406, 2012.

---

[6]The first is targeted therapy on the mutated pathways, as we mentioned in the Introduction. The second is cancer prevention through identifying preventable carcinogens.

[6] R. Dridi and H. Alghassi. Homology computation of large point clouds using quantum annealing. Arxiv:1512.09328. 2015.

[7] D. Hanahan and R. A. Weinberg. The hallmarks of cancer. *Cell*, 100(1):57–70, 2016.

[8] M. W. Johnson, M. H. S. Amin, S. Gildert, T. Lanting, F. Hamze, N. Dickson, R. Harris, A. J. Berkley, J. Johansson, P. Bunyk, E. M. Chapple, C. Enderud, J. P. Hilton, K. Karimi, E. Ladizinsky, N. Ladizinsky, T. Oh, I. Perminov, C. Rich, M. C. Thom, E. Tolkacheva, C. J. S. Truncik, S. Uchaikin, J. Wang, B. Wilson, and G. Rose. Quantum annealing with manufactured spins. *Nature*, 473(7346):194–198, 05 2011.

[9] M. D. Leiserson, H.-T. Wu, F. Vandin, and B. J. Raphael. CoMEt: a statistical approach to identify combinations of mutually exclusive alterations in cancer. *Genome Biology*, 16(1):160, 2015.

[10] M. D. M. Leiserson, H.-T. Wu, F. Vandin, and B. J. Raphael. Comet: A statistical approach to identify combinations of mutually exclusive alterations in cancer. In T. M. Przytycka, editor, *Research in Computational Molecular Biology*, 2015.

[11] P. Y. Lum, G. Singh, A. Lehman, T. Ishkanov, M. Vejdemo-Johansson, M. Alagappan, J. Carlsson, and G. Carlsson. Extracting insights from the shape of complex data using topology. *Scientific Reports*, 3:1236 EP –, 02 2013.

[12] J. Lurie. *Higher Topos Theory (AM-170)*. Princeton University Press, 2009.

[13] T. C. G. A. R. Network. Comprehensive genomic characterization defines human glioblastoma genes and core pathways. *Nature*, 455(7216):1061–1068, 2008.

[14] T. C. G. A. R. Network. Genomic and epigenomic landscapes of adult de novo acute myeloid leukemia. *New England Journal of Medicine*, 368(22):2059–2074, 2013.

[15] M. Nicolau, A. J. Levine, and G. Carlsson. Topology based data analysis identifies a subgroup of breast cancers with a unique mutational profile

and excellent survival. *Proceedings of the National Academy of Sciences of the United States of America*, 108 17:7265–70, 2011.

[16] P. A. Northcott, I. Buchhalter, A. S. Morrissy, V. Hovestadt, J. Weischenfeldt, T. Ehrenberger, S. Gröbner, M. Segura-Wang, T. Zichner, V. A. Rudneva, H.-J. Warnatz, N. Sidiropoulos, A. H. Phillips, S. Schumacher, K. Kleinheinz, S. M. Waszak, S. Erkek, D. T. W. Jones, B. C. Worst, M. Kool, M. Zapatka, N. Jäger, L. Chavez, B. Hutter, M. Bieg, N. Paramasivam, M. Heinold, Z. Gu, N. Ishaque, C. Jäger-Schmidt, C. D. Imbusch, A. Jugold, D. Hübschmann, T. Risch, V. Amstislavskiy, F. G. R. Gonzalez, U. D. Weber, S. Wolf, G. W. Robinson, X. Zhou, G. Wu, D. Finkelstein, Y. Liu, F. M. G. Cavalli, B. Luu, V. Ramaswamy, X. Wu, J. Koster, M. Ryzhova, Y.-J. Cho, S. L. Pomeroy, C. Herold-Mende, M. Schuhmann, M. Ebinger, L. M. Liau, J. Mora, R. E. McLendon, N. Jabado, T. Kumabe, E. Chuah, Y. Ma, R. A. Moore, A. J. Mungall, K. L. Mungall, N. Thiessen, K. Tse, T. Wong, S. J. M. Jones, O. Witt, T. Milde, A. Von Deimling, D. Capper, A. Korshunov, M.-L. Yaspo, R. Kriwacki, A. Gajjar, J. Zhang, R. Beroukhim, E. Fraenkel, J. O. Korbel, B. Brors, M. Schlesner, R. Eils, M. A. Marra, S. M. Pfister, M. D. Taylor, and P. Lichter. The whole-genome landscape of medulloblastoma subtypes. *Nature*, 547:311 EP –, 07 2017.

[17] N. Riaz, P. Blecua, R. S. Lim, R. Shen, D. S. Higginson, N. Weinhold, L. Norton, B. Weigelt, S. N. Powell, and J. S. Reis-Filho. Pan-cancer analysis of bi-allelic alterations in homologous recombination dna repair genes. *Nature Communications*, 8(1):857, 2017.

[18] E. Szczurek and N. Beerenwinkel. Modeling mutual exclusivity of cancer mutations. In R. Sharan, editor, *Research in Computational Molecular Biology*, 2014.

[19] The Univalent Foundations Program. *Homotopy Type Theory: Univalent Foundations of Mathematics*. https://homotopytypetheory.org/book, Institute for Advanced Study, 2013.

[20] J. van de Haar, S. Canisius, M. K. Yu, E. E. Voest, L. F. Wessels, and T. Ideker. Identifying epistasis in cancer genomes: A delicate affair. *Cell*, 177(6):1375 – 1383, 2019.

18

[21] F. Vandin, P. Clay, E. Upfal, and B. J. Raphael. Discovery of mutated subnetworks associated with clinical data in cancer. In *Biocomputing 2012: Proceedings of the Pacific Symposium, Kohala Coast, Hawaii, USA, January 3-7, 2012*, pages 55–66, 2012.

[22] F. Vandin, E. Upfal, and B. Raphael. De novo discovery of mutated driver pathways in cancer. *Genome Research*, 22(2):375–385, 2012.

[23] F. Vandin, E. Upfal, and B. J. Raphael. De novo discovery of mutated driver pathways in cancer. *Genome Research*, 22(2):375–385, 2012.

[24] B. Vogelstein and K. W. Kinzler. Cancer genes and the pathways they control. *Nat Med*, 10(8):789–799, 2004.

[25] R. Weinberg. *The Biology of Cancer*. W. W. Norton & Company, 2013.

[26] C.-H. Yeang, F. McCormick, and A. Levine. Combinatorial patterns of somatic gene mutations in cancer. *The FASEB Journal*, 22(8):2605–2622, 2008.

[27] A. Zomorodian and G. Carlsson. Localized homology. *Computational Geometry*, 41(3):126 – 148, 2008.

A Appendix

This appendix has three parts. In the first part, we review an efficient procedure for computing homology groups. The remaining two parts give the obtained list of pathways for GBM and AML data, respectively.

A.1 Computing homology on quantum computers

We provide the following material (from [6]) for easy access. We review how the homology spaces $H_*(X)$ are computed. In principle, the formal definitions of homology that can be found in any algebraic topology textbook, are sufficient for computations. However, we point here to a more efficient approach based on Mayer-Vietoris blow-up complexes. We formulate finding optimal Mayer-Vietoris blow-up complexes as Quadratic Unconstrained Binary Optimizations (QUBO). QUBO-solvers (such as the D-Wave quantum annealer [8] or quantum-inspired classical solvers such as [2]) are now available for calculations.

Let $\mathcal{C} = \{K^i\}_{i \in I}$ be a cover of K by simplicial subcomplexes $K^i \subseteq K$; here again we have dropped the subscript ε from K_ε for simplicity. For $J \subseteq I$, we define $K^J = \cap_{j \in J} K^j$.

Definition 5 *The* Mayer-Vietoris blow-up complex *of the simplicial complex K and cover $\mathcal{C}$, is defined by:*

$$K^{\mathcal{C}} = \bigcup_{J \subseteq I} \bigcup_{\sigma \in K^J} \sigma \times J.$$

A basis for the $k-$chains $C_k(K^{\mathcal{C}})$ is $\{\sigma \otimes J \in K^{\mathcal{C}} | \dim \sigma + \operatorname{card} J = n\}$. The boundary of a cell $\sigma \otimes J$ is given by: $\partial(\sigma \otimes J) = \partial \sigma \otimes J + (-1)^{\dim \sigma} \sigma \otimes \partial J.$

Simply put, the simplicial complex $K^{\mathcal{C}}$ is the set of the "original" simplices in addition to the ones we get by blowing up common simplices. These are of the form $\sigma \otimes J$ in the definition above. In Figure 6, the yellow vertex d common to the two subcomplexes $\{K_1, K_2\}$ is blown-up into an edge $d \otimes 12$, and the edge bc is blown-up into the "triangle" $bc \otimes 01$. In Figure 7, the vertex a common to three subcomplexes $\{K_0, K_1, K_2\}$ is blown-up into the triangle $a \otimes 012$.

We will not prove it here, but the projection $K^{\mathcal{C}} \to K$ is a homotopy equivalence and induces an isomorphism $H_*(K^{\mathcal{C}}) \simeq H_*(K)$ [27]. The key

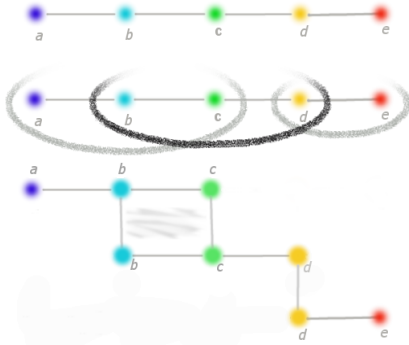Figure 6: (Top) The simplicial complex K is the depicted graph. (Middle) K is covered with K_0, K_1, and K_2. (Bottom) The blow-up complex of the cover depicted in the middle picture. After the blow-up, the edges $b \otimes 01$, $c \otimes 01$, $d \otimes 12$, and the triangle $bc \otimes 01$ appear.
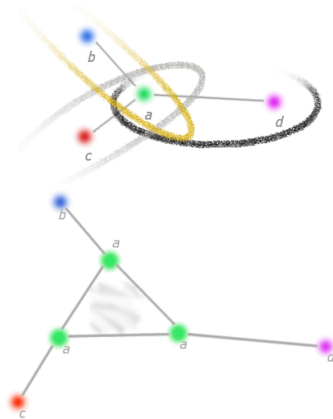

Figure 7: The triangle $a \times 012$ appears after blowing-up the cover of the middle picture.

point is that the boundary map of the simplicial complex $K^{\mathcal{C}}$ (which replaces K by the homotopy equivalence) has a nice block form suitable for parallel rank computation. As an example, let us consider again the simplicial complex K depicted in Figure 6. First, $C_0(K^{\mathcal{C}})$, the space of vertices of the blow-up complex $K^{\mathcal{C}}$, is spanned by the vertices

$$\{a \otimes 0,\ b \otimes 0,\ c \otimes 0,\ b \otimes 1,\ c \otimes 1,\ d \otimes 1,\ d \otimes 2,\ e \otimes 2\},$$

that is, all vertices of K taking into account the partition they belong to. The space of edges $C_1(K^{\mathcal{C}})$ is spanned by

$$\{ab \otimes 0, bc \otimes 0, bc \otimes 1, cd \otimes 1, de \otimes 2, b \otimes 01,\ c \otimes 01,\ d \otimes 12\},$$

which is the set of the "original" edges (edges of the form $\sigma \otimes j$ with $j \in J = \{0,1,2\}$ and σ is an edge in K) and the new ones resulting from blow-ups, that is, those of the form $v \otimes ij$ where v is a vertex in $K^j \cap K^j$ (if the intersection is empty, the value of boundary map is just 0). The matrix of the boundary map ∂_0 with respect to the given ordering is then:

$$\partial_0 = \begin{pmatrix}
-1 & 0 & 0 & 0 & 0 & 0 & 0 & 0 \\
1 & -1 & 0 & 0 & 0 & -1 & 0 & 0 \\
0 & 1 & 0 & 0 & 0 & 0 & -1 & 0 \\
0 & 0 & -1 & 0 & 0 & 1 & 0 & 0 \\
0 & 0 & 1 & -1 & 0 & 0 & 1 & 0 \\
0 & 0 & 0 & 1 & 0 & 0 & 0 & -1 \\
0 & 0 & 0 & 0 & -1 & 0 & 0 & 1 \\
0 & 0 & 0 & 0 & 1 & 0 & 0 & 0
\end{pmatrix}$$

Clearly, one can now row-reduce each coloured block independently. There might be *remainders*, that is, zero rows except for the intersection part. We collect all such rows in one extra matrix and row-reduce it at the end and aggregate. For the second boundary matrix we need to determine $C_2(K^{\mathcal{C}})$. The 2-simplices are of three forms. First, the original ones (those of the form $\sigma \otimes j$ with $\sigma \in C_2(K)$; in this example there is none) then those of the form $\sigma \times \{i,j\}$, with σ being in $K^i \cap K^j$. And finally, those of the form $v \otimes \{i,j,k\}$, with $v \in K^i \cap K^j \cap K^k$ (there is none in this example, but Figure 5 has one). We get $C_2(K^{\mathcal{C}}) = \langle bc \otimes 01 \rangle$; thus, there is no need for parallel computation.

Finally, for efficient computations, it is necessary that the homologies of the smaller blocks are easy to compute. This is where the QUBO-solver comes

in. It is used to obtain a "good" cover $\mathcal{C}$ by computing a clique cover of the original graph G (plus a completion step). It is easy to see that such coverings do, indeed, come with trivial block homologies [6].

A.2 GBM pathways list

The table below reports the final pathways in Figure 5. Details on the data, the parameters, and how the pathways are computed using persistent homology, can be found in Subsection 4.2 on page 13.

Pathway	coverage η
RB1 , NF1 , CYP27B1 , CDKN2B	70
RB1 , NF1 , MDM2 , AVIL-CTDSP2 , CDKN2B	69
TP53 , MDM2 , OS9 , CDKN2A	69
TP53 , MDM2 , AVIL-CTDSP2 , CDKN2A	69
TP53 , MDM2 , DTX3 , CDKN2A	69
RB1 , NF1 , CDK4 , CDKN2B	69
RB1 , NF1 , MDM2 , OS9 , CDKN2B	68
TP53 , MDM2 , OS9 , MTAP	68
TP53 , MDM2 , AVIL-CTDSP2 , MTAP	68
TP53 , MDM2 , DTX3 , MTAP	68
TP53 , CDK4 , CDKN2A	68
TP53 , CYP27B1 , CDKN2A	68
TP53 , CDK4 , MTAP	67
TP53 , CYP27B1 , MTAP	67
RB1 , NF1 , CYP27B1 , CDKN2A	66
RB1 , NF1 , MDM2 , OS9 , CDKN2A	65
RB1 , NF1 , MDM2 , AVIL-CTDSP2 , CDKN2A	65
RB1 , NF1 , MDM2 , DTX3 , CDKN2B	65
RB1 , NF1 , CDK4 , CDKN2A	65
RB1 , NF1 , CYP27B1 , MTAP	65
RB1 , NF1 , MDM2 , OS9 , MTAP	64
RB1 , NF1 , MDM2 , AVIL-CTDSP2 , MTAP	64
RB1 , NF1 , CDK4 , MTAP	64
RB1 , NF1 , MDM2 , DTX3 , CDKN2A	62
RB1 , NF1 , MDM2 , DTX3 , MTAP	61
TP53 , MDM2 , AVIL-CTDSP2 , SEC61G	60
RB1 , NF1 , EGFR , OS9	60
TP53 , MDM2 , OS9 , SEC61G	59
TP53 , MDM2 , DTX3 , SEC61G	59
PTEN , IFNA21 , MDM2 , AVIL-CTDSP2	58
TP53 , MDM2 , AVIL-CTDSP2 , IFNA21	58
RB1 , NF1 , EGFR , DTX3	58
PTEN , IFNA21 , CYP27B1	58
PTEN , IFNA21 , MDM2 , OS9	57
TP53 , MDM2 , OS9 , IFNA21	57
TP53 , MDM2 , DTX3 , IFNA21	57
PTEN , IFNA21 , CDK4	57
RB1 , NF1 , MDM2 , AVIL-CTDSP2 , SEC61G	55

PTEN , IFNA21 , MDM2 , DTX3	55
TP53 , MDM2 , AVIL-CTDSP2 , ELAVL2	55
RB1 , NF1 , MDM2 , OS9 , SEC61G	54
TP53 , MDM2 , OS9 , ELAVL2	54
TP53 , MDM2 , DTX3 , ELAVL2	54
RB1 , NF1 , MDM2 , AVIL-CTDSP2 , IFNA21	53
TP53 , CDK4 , IFNA21	53
TP53 , CDK4 , ELAVL2	53
TP53 , CYP27B1 , IFNA21	53
TP53 , CYP27B1 , ELAVL2	53
RB1 , NF1 , MDM2 , OS9 , IFNA21	52
RB1 , NF1 , MDM2 , DTX3 , SEC61G	52
RB1 , NF1 , MDM2 , AVIL-CTDSP2 , ELAVL2	51
RB1 , NF1 , CYP27B1 , IFNA21	51
RB1 , NF1 , CYP27B1 , ELAVL2	51
RB1 , NF1 , MDM2 , OS9 , ELAVL2	50
RB1 , NF1 , CDK4 , IFNA21	50
RB1 , NF1 , CDK4 , ELAVL2	50
RB1 , NF1 , MDM2 , DTX3 , IFNA21	49
RB1 , NF1 , MDM2 , DTX3 , ELAVL2	47

A.3 AML pathways list

The following table gives the list of all 65 pathways of $\mathcal{N}_1$ (Figure 4) and their coverage. Details about the data and how the pathways are obtained using persistent homology can be found in Section 3.1. All pathways listed below passed our robustness test.

Pathway	Coverage
PML.RARA , MYH11.CBFB , RUNX1.RUNX1T1 , TP53 , NPM1 , RUNX1	123
PML.RARA , MYH11.CBFB , RUNX1.RUNX1T1 , TP53 , NPM1 , MLL.PTD	113
PML.RARA , MYH11.CBFB , RUNX1.RUNX1T1 , DNMT3A	85
Other Tyr kinases , MYH11.CBFB , MLL.PTD , NPM1	83
MLL-X fusions , TP53 , FLT3	81
Other Tyr kinases , MYH11.CBFB , DNMT3A , MLL-X fusions	80
PML.RARA , MYH11.CBFB , Cohesin , Other modifiers	78
MLL-X fusions , DNMT3A , RUNX1.RUNX1T1 , MYH11.CBFB	78
PML.RARA , MYH11.CBFB , RUNX1.RUNX1T1 , TP53 , PHF6 , IDH1	75
Other myeloid TFs , MYH11.CBFB , Cohesin , Other modifiers	74
Other Tyr kinases , FLT3 , MLL-X fusions	74
PML.RARA , MYH11.CBFB , RUNX1.RUNX1T1 , TP53 , IDH2	70
PML.RARA , MYH11.CBFB , RUNX1.RUNX1T1 , CEBPA , RUNX1	66
PML.RARA , MYH11.CBFB , RUNX1.RUNX1T1 , TP53 , PHF6 , MLL.PTD	65
Other myeloid TFs , MYH11.CBFB , TP53 , RUNX1.RUNX1T1 , RUNX1	65
PML.RARA , PTPs , IDH2 , TET2	65
PML.RARA , MYH11.CBFB , TET2 , IDH2	64
MLL-X fusions , TP53 , RUNX1.RUNX1T1 , MYH11.CBFB , IDH2	63
PML.RARA , MYH11.CBFB , RUNX1.RUNX1T1 , CEBPA , PHF6 , MLL.PTD	62
PML.RARA , KRAS/NRAS , PHF6 , MLL.PTD , KIT	62
MLL-X fusions , TP53 , RUNX1.RUNX1T1 , MYH11.CBFB , IDH1	62
MLL-X fusions , TP53 , RUNX1.RUNX1T1 , MYH11.CBFB , RUNX1	62
Other myeloid TFs , MYH11.CBFB , TP53 , RUNX1.RUNX1T1 , PHF6 , MLL.PTD	61
PML.RARA , KRAS/NRAS , PHF6 , MLL.PTD , RUNX1.RUNX1T1	61
PML.RARA , KIT , TP53 , IDH2	60
PML.RARA , KIT , TP53 , RUNX1	59
MLL-X fusions , TET2 , MYH11.CBFB , IDH2	57
PML.RARA , PTPs , IDH2 , KIT	56
PML.RARA , KIT , CEBPA , RUNX1	56
PML.RARA , KIT , TP53 , PHF6 , MLL.PTD	55
PML.RARA , PTPs , IDH2 , RUNX1.RUNX1T1	55
PML.RARA , PTPs , RUNX1 , KIT	55
Other myeloid TFs , KIT , TP53 , RUNX1	55
PML.RARA , PTPs , RUNX1 , RUNX1.RUNX1T1	54
MLL-X fusions , TP53 , KIT , IDH2	53
PML.RARA , KIT , CEBPA , PHF6 , MLL.PTD	52
MLL-X fusions , TP53 , RUNX1.RUNX1T1 , MYH11.CBFB , MLL.PTD	52
Ser-Tyr kinases , RUNX1.RUNX1T1 , PTPs , MLL.PTD	52
MLL-X fusions , TP53 , KIT , RUNX1	52

Pathway	Coverage
Other myeloid TFs , KIT , TP53 , PHF6 , MLL.PTD	51
PML.RARA , WT1 , RUNX1.RUNX1T1 , TP53	51
PML.RARA , MYH11.CBFB , TET2 , PHF6	50
PML.RARA , KIT , Cohesin	50
Other Tyr kinases , MYH11.CBFB , IDH2 , MLL-X fusions	49
Other Tyr kinases , MYH11.CBFB , IDH1 , MLL-X fusions	48
Other Tyr kinases , MYH11.CBFB , MLL.PTD , PHF6 , Other myeloid TFs	47
Other Tyr kinases , KRAS/NRAS , PHF6 , MLL.PTD	47
Other myeloid TFs , MYH11.CBFB , TET2 , PHF6	46
MLL-X fusions , Cohesin , MYH11.CBFB	46
Other myeloid TFs , KIT , Cohesin	46
Other Tyr kinases , MYH11.CBFB , IDH1 , PHF6	45
PML.RARA , PTPs , MLL.PTD , KIT	45
PML.RARA , WT1 , TET2	45
PML.RARA , PTPs , MLL.PTD , RUNX1.RUNX1T1	44
MLL-X fusions , TP53 , RUNX1.RUNX1T1 , WT1	44
MLL-X fusions , Cohesin , KIT	43
MLL-X fusions , TP53 , KIT , MLL.PTD	42
Other Tyr kinases , PTPs , IDH2	41
Other Tyr kinases , MYH11.CBFB , MLL.PTD , MLL-X fusions	38
MLL-X fusions , TET2 , WT1	38
Spliceosome , CEBPA	37
Spliceosome , PTPs	36
Spliceosome , Other myeloid TFs	36
Other Tyr kinases , WT1 , MLL-X fusions	30
Other Tyr kinases , PTPs , MLL.PTD	30

The following long table gives the assignment *tumor ↦ list of pathways* for the AML data. For each tumor we assign a robust (in our topological sense) set of pathways. More specifically, for a tumor (sample ID) i, the second column gives the list of all pathways that have passed our robustness test.

Sample ID	Pathways	Cyto
0	0, 1, 2, 6, 8, 11, 12, 13, 15, 16, 18, 19, 23, 24, 25, 27, 28, 29, 30, 31, 33, 35, 40, 41, 42, 51, 52, 53	Good
1	0, 1, 2, 7, 8, 11, 12, 13, 14, 17, 18, 20, 21, 22, 23, 30, 33, 36, 37, 40, 53, 54	Good
2	0, 1, 2, 3, 4, 5, 6, 7, 8, 9, 10, 11, 12, 13, 14, 16, 17, 18, 19, 20, 21, 22, 23, 26, 36, 41, 43, 44, 45, 46, 47, 48, 50, 58	Good
3	0, 1, 2, 3, 5, 6, 7, 8, 9, 11, 12, 13, 14, 16, 17, 18, 20, 21, 22, 26, 36, 41, 43, 44, 45, 47, 48, 50, 58	Good
4	0, 1, 2, 3, 5, 6, 8, 10, 11, 12, 13, 15, 16, 18, 19, 23, 24, 25, 27, 28, 29, 30, 31, 33, 35, 40, 41, 42, 43, 44, 45, 46, 50, 51, 52, 53, 57, 58, 63, 64	Good
5	0, 1, 2, 4, 6, 8, 10, 11, 12, 13, 15, 16, 18, 19, 23, 24, 25, 27, 28, 29, 30, 31, 33, 35, 40, 41, 42, 51, 52, 53	Good
6	0, 1, 2, 3, 5, 6, 7, 8, 9, 11, 12, 13, 14, 15, 16, 17, 18, 20, 21, 22, 26, 27, 30, 31, 33, 36, 37, 41, 43, 44, 45, 47, 48, 50, 51, 53, 57, 58, 61, 64	Good
7	0, 1, 2, 3, 5, 6, 7, 8, 9, 10, 11, 12, 13, 14, 17, 18, 19, 20, 21, 22, 23, 24, 25, 27, 28, 29, 30, 31, 32, 33, 34, 35, 36, 37, 38, 39, 40, 42, 43, 44, 45, 46, 49, 50, 51, 53, 54, 55, 56, 57, 58, 60, 61, 62, 63, 64	Good
8	0, 1, 2, 4, 7, 8, 10, 11, 12, 13, 14, 17, 18, 20, 21, 22, 23, 30, 33, 36, 37, 40, 53, 54	Good
9	0, 1, 2, 6, 8, 11, 12, 13, 15, 16, 18, 19, 23, 24, 25, 27, 28, 29, 30, 31, 33, 35, 40, 41, 42, 51, 52, 53	Good
10	0, 1, 2, 3, 5, 6, 7, 8, 9, 11, 12, 13, 14, 16, 17, 18, 20, 21, 22, 26, 36, 41, 43, 44, 45, 47, 48, 50, 58	Good
11	0, 1, 2, 6, 8, 11, 12, 13, 15, 16, 18, 19, 23, 24, 25, 27, 28, 29, 30, 31, 33, 35, 40, 41, 42, 51, 52, 53, 60, 61, 62	Good
12	40, 52, 54, 59, 60, 61, 62, 63	Good
13	0, 1, 2, 3, 5, 6, 7, 8, 9, 11, 12, 13, 14, 16, 17, 18, 19, 20, 21, 22, 24, 25, 26, 27, 28, 29, 31, 32, 34, 35, 36, 38, 39, 41, 42, 43, 44, 45, 47, 48, 49, 50, 51, 55, 56, 58	Good
14	0, 1, 2, 4, 6, 8, 10, 11, 12, 13, 15, 16, 18, 19, 23, 24, 25, 27, 28, 29, 30, 31, 33, 35, 40, 41, 42, 51, 52, 53	Good
15	0, 1, 2, 6, 8, 11, 12, 13, 15, 16, 18, 19, 23, 24, 25, 27, 28, 29, 30, 31, 33, 35, 40, 41, 42, 51, 52, 53	Good
16	0, 1, 2, 3, 5, 6, 7, 8, 9, 10, 11, 12, 13, 14, 17, 18, 20, 21, 22, 26, 27, 30, 31, 33, 36, 37, 41, 43, 44, 45, 46, 48, 49, 50, 53, 54, 55, 57, 58, 63, 64	Good
17	0, 1, 2, 4, 6, 8, 10, 11, 12, 13, 15, 16, 18, 19, 23, 24, 25, 27, 28, 29, 30, 31, 33, 35, 40, 41, 42, 51, 52, 53	Good
18	0, 1, 2, 3, 5, 6, 7, 8, 9, 11, 12, 13, 14, 16, 17, 18, 19, 20, 21, 22, 24, 25, 26, 27, 28, 29, 31, 32, 34, 35, 36, 37, 38, 39, 41, 42, 43, 44, 45, 47, 48, 49, 50, 51, 55, 56, 58, 60, 61, 62	Good
19	0, 1, 2, 6, 8, 11, 12, 13, 15, 16, 18, 19, 23, 24, 25, 27, 28, 29, 30, 31, 33, 35, 40, 41, 42, 51, 52, 53	Good
20	0, 1, 2, 3, 5, 6, 7, 8, 9, 11, 12, 13, 14, 16, 17, 18, 20, 21, 22, 26, 36, 41, 43, 44, 45, 47, 48, 50, 58	Good
21	0, 1, 2, 7, 8, 11, 12, 13, 14, 15, 16, 17, 18, 19, 20, 21, 22, 23, 24, 25, 26, 27, 28, 29, 30, 31, 32, 33, 34, 35, 36, 37, 38, 39, 40, 41, 42, 47, 49, 51, 52, 53, 54, 55, 56, 59, 60, 61, 62	Good
22	32, 4, 39, 9, 10, 45, 14, 47, 49, 22, 62	Good
23	0, 1, 2, 6, 8, 11, 12, 13, 15, 16, 18, 19, 23, 24, 25, 27, 28, 29, 30, 31, 33, 35, 40, 41, 42, 51, 52, 53	Good
24	0, 1, 2, 3, 4, 5, 6, 7, 8, 9, 10, 11, 12, 13, 14, 16, 17, 18, 20, 21, 22, 26, 36, 41, 43, 44, 45, 47, 48, 50, 58	Good
25	0, 1, 2, 3, 5, 6, 7, 8, 9, 11, 12, 13, 14, 16, 17, 18, 19, 20, 21, 22, 24, 25, 26, 27, 28, 29, 31, 32, 34, 35, 36, 38, 39, 40, 41, 42, 43, 44, 45, 47, 48, 49, 50, 51, 52, 54, 55, 56, 58, 59, 63	Good
26	0, 1, 2, 3, 5, 6, 7, 8, 9, 11, 12, 13, 14, 16, 17, 18, 19, 20, 21, 22, 23, 26, 36, 41, 43, 44, 45, 46, 47, 48, 50, 58	Good
27	0, 1, 2, 6, 8, 9, 11, 12, 13, 14, 15, 16, 18, 19, 22, 23, 24, 25, 27, 28, 29, 30, 31, 32, 33, 35, 39, 40, 41, 42, 45, 47, 49, 51, 52, 53, 62	Good
28	0, 1, 2, 4, 6, 8, 10, 11, 12, 13, 15, 16, 18, 19, 23, 24, 25, 27, 28, 29, 30, 31, 33, 35, 40, 41, 42, 51, 52, 53	Good
29	0, 1, 2, 6, 7, 8, 9, 11, 12, 13, 14, 17, 18, 20, 21, 22, 23, 30, 33, 36, 37, 40, 42, 48, 49, 53, 54, 55	Good
30	0, 1, 2, 4, 5, 6, 7, 8, 10, 11, 12, 13, 15, 16, 17, 18, 19, 20, 21, 23, 24, 25, 26, 27, 28, 29, 30, 31, 33, 34, 35, 36, 38, 40, 41, 42, 43, 44, 48, 51, 52, 53, 54, 55, 56, 58, 59, 63	Good
31	37	Good
32	0, 1, 2, 3, 5, 6, 7, 8, 9, 11, 12, 13, 14, 16, 17, 18, 20, 21, 22, 26, 36, 41, 43, 44, 45, 47, 48, 50, 58	Good
33	0, 1, 2, 3, 5, 6, 8, 10, 11, 12, 13, 15, 16, 18, 19, 23, 24, 25, 27, 28, 29, 30, 31, 33, 35, 40, 41, 42, 43, 44, 45, 46, 50, 51, 52, 53, 57, 58, 63, 64	Good
34	0, 1, 2, 6, 7, 8, 9, 11, 12, 13, 14, 17, 18, 20, 21, 22, 23, 30, 33, 36, 37, 40, 42, 48, 49, 53, 54, 55	Good
35	0, 1, 2, 4, 6, 8, 10, 11, 12, 13, 15, 16, 18, 19, 23, 24, 25, 27, 28, 29, 30, 31, 33, 35, 40, 41, 42, 51, 52, 53	Good
36	10, 4	Good
37	0, 1, 2, 3, 5, 7, 8, 64, 44, 61, 15, 50, 51, 20, 53, 57, 33, 27, 37, 30, 31	Intermediate
38	35, 6, 39, 8, 41, 13, 46, 45, 50, 18, 19, 9, 22, 23, 47, 29	Intermediate
39	0, 32, 34, 43, 38, 33, 11, 12, 14, 15, 16, 17, 21, 25, 24, 57, 26, 27, 28, 30, 31	Intermediate
40	0, 11, 12, 14, 15, 16, 17, 21, 24, 25, 26, 27, 28, 30, 31, 32, 33, 34, 37, 38, 43, 57	Intermediate
41	35, 60, 12, 46, 18, 19, 23, 28	Intermediate
42	0, 1, 2, 3, 5, 7	Intermediate
43	0, 1, 2, 3, 4, 5, 6, 7, 9, 10, 48, 49, 55, 42	Intermediate
44	0, 6, 9, 12, 14, 15, 16, 19, 21, 23, 25, 26, 28, 31, 32, 33, 38, 41, 42, 46, 47, 48, 49, 52, 55, 59, 60, 61, 62	Intermediate
45	0, 1, 10, 3, 4	Intermediate
46	2, 43, 5, 7, 11, 34, 46, 15, 16, 17, 19, 23, 24, 57, 26, 27, 30, 37	Intermediate
47	10, 4	Intermediate
48	0, 1, 3, 4, 6, 9, 10, 15, 27, 30, 31, 33, 37, 42, 48, 49, 51, 53, 55, 57, 61, 64	Intermediate
49	0, 1, 2, 3, 4, 5, 7, 10	Intermediate
50	0, 1, 2, 3, 4, 5, 7, 41, 10, 15, 16, 59, 52, 26, 47	Intermediate
51	0, 1, 3, 4, 6, 9, 10, 15, 27, 30, 31, 33, 37, 42, 48, 49, 51, 53, 55, 57, 61, 64	Intermediate
52	0, 1, 3, 37, 6, 33, 64, 9, 42, 15, 48, 49, 51, 53, 55, 57, 27, 61, 30, 31	Intermediate
53	2, 59, 5, 7, 41, 15, 16, 52, 26, 47	Intermediate
54	0, 1, 2, 3, 4, 5, 7, 10, 46, 19, 23	Intermediate
55	0, 1, 2, 3, 4, 5, 6, 7, 9, 10, 48, 49, 55, 42	Intermediate
56	0, 1, 2, 3, 4, 5, 7, 10	Intermediate
57	1, 3, 8, 13, 18, 19, 20, 22, 23, 29, 35, 36, 37, 39, 44, 45, 46, 50, 51, 53, 56, 58, 64	Intermediate
58	0, 2, 5, 6, 7, 8, 9, 12, 13, 14, 18, 19, 21, 22, 23, 25, 28, 29, 31, 32, 33, 35, 37, 38, 39, 41, 42, 45, 46, 47, 48, 49, 50, 55, 60, 61, 62	Intermediate
59	2, 5, 7, 46, 19, 23, 60, 61, 62	Intermediate
60	0, 1, 3, 4, 6, 9, 10, 48, 49, 55, 42	Intermediate
61	0, 1, 3, 4, 6, 40, 9, 10, 48, 49, 52, 54, 55, 59, 42, 63	Intermediate
62	10, 4	Intermediate
63	28, 18, 35, 12, 60	Intermediate
64	0, 8, 11, 12, 14, 15, 16, 17, 20, 21, 24, 25, 26, 27, 28, 30, 31, 32, 33, 34, 38, 43, 44, 50, 57, 60, 61, 62	Intermediate
65	48, 2, 59, 5, 6, 7, 8, 41, 42, 55, 44, 15, 16, 49, 50, 52, 9, 20, 26, 47	Intermediate
66	32, 2, 5, 7, 9, 39, 45, 14, 47, 49, 22, 62	Intermediate
67	0, 1, 2, 3, 5, 6, 7, 9, 42, 48, 49, 55	Intermediate
68	0, 1, 2, 3, 4, 5, 7, 10	Intermediate
69	0, 1, 2, 3, 5, 6, 7, 40, 9, 44, 8, 50, 52, 54, 20, 59, 63	Intermediate
70	0, 1, 34, 3, 11, 46, 15, 16, 17, 19, 43, 23, 24, 57, 26, 27, 30	Intermediate
71	32, 39, 9, 45, 14, 47, 49, 22, 62	Intermediate
72	0, 1, 34, 3, 4, 10, 11, 15, 16, 17, 43, 24, 57, 26, 27, 30	Intermediate
73	0, 1, 3, 8, 44, 50, 20	Intermediate
74	0, 1, 3, 4, 41, 10, 15, 16, 59, 52, 26, 47	Intermediate
75	35, 4, 60, 10, 12, 18, 28	Intermediate
76	0, 1, 2, 3, 4, 5, 7, 10	Intermediate
77	1, 2, 3, 4, 5, 6, 7, 9, 10, 13, 15, 16, 18, 19, 22, 23, 26, 29, 35, 36, 37, 39, 41, 45, 46, 47, 51, 52, 53, 56, 58, 59, 64	Intermediate
78	10, 4	Intermediate
79	2, 5, 7	Intermediate
80	0, 1, 2, 3, 4, 5, 7, 9, 10, 39, 45, 14, 47, 49, 32, 22, 62	Intermediate
81	34, 4, 5, 38, 7, 10, 43, 44, 48, 17, 20, 21, 54, 55, 56, 36, 26, 59, 58, 63	Intermediate
82	4, 6, 8, 9, 10, 44, 50, 20	Intermediate
83	2, 5, 7, 9, 14, 15, 22, 27, 30, 31, 32, 33, 37, 39, 45, 47, 49, 51, 53, 57, 61, 62, 64	Intermediate

84	0, 1, 3, 4, 10, 12, 13, 14, 18, 19, 21, 22, 23, 25, 28, 29, 31, 32, 33, 35, 36, 37, 38, 39, 40, 45, 46, 51, 52, 53, 54, 56, 58, 59, 63, 64	Intermediate
85	9, 10, 4, 6	Intermediate
86	0, 1, 3	Intermediate
87	0, 1, 10, 3, 4	Intermediate
88	34, 43, 37, 11, 15, 16, 17, 62, 24, 57, 26, 27, 60, 61, 30	Intermediate
89	0, 1, 3	Intermediate
90	0, 1, 2, 3, 5, 7, 8, 64, 44, 61, 15, 50, 51, 20, 53, 57, 33, 27, 37, 30, 31	Intermediate
91	0, 1, 2, 3, 5, 6, 7, 9, 12, 15, 18, 19, 23, 27, 28, 30, 31, 33, 35, 37, 40, 42, 46, 48, 49, 51, 52, 53, 54, 55, 57, 59, 60, 61, 63, 64	Intermediate
92	0, 32, 34, 43, 38, 33, 11, 12, 14, 15, 16, 17, 21, 25, 24, 57, 26, 27, 28, 30, 31	Intermediate
93	59, 37, 41, 47, 16, 52, 26, 15, 60, 61, 62	Intermediate
94	0, 1, 2, 3, 4, 5, 7, 8, 9, 10, 39, 44, 45, 14, 47, 49, 50, 20, 32, 22, 62	Intermediate
95	0, 1, 2, 3, 5, 6, 7, 9, 42, 55, 46, 48, 49, 19, 23	Intermediate
96	0, 32, 38, 33, 12, 14, 21, 25, 28, 31	Intermediate
97	59, 41, 46, 47, 16, 19, 52, 23, 26, 15	Intermediate
98	0, 1, 10, 3, 4	Intermediate
99	0, 1, 3, 37, 8, 44, 50, 20	Intermediate
100	0, 1, 2, 4, 5, 7, 8, 11, 13, 14, 17, 20, 21, 22, 24, 25, 29, 32, 34, 36, 37, 38, 39, 40, 54, 56	Intermediate
101	28, 18, 35, 12, 60	Intermediate
102	0, 1, 3, 8, 44, 50, 20	Intermediate
103	0, 32, 38, 33, 12, 14, 21, 25, 28, 31	Intermediate
104	34, 4, 5, 38, 7, 10, 43, 44, 48, 17, 20, 21, 54, 55, 56, 36, 26, 59, 58, 63	Intermediate
105	32, 51, 34, 35, 38, 39, 60, 42, 61, 49, 19, 56, 55, 24, 25, 27, 28, 29, 62, 31	Intermediate
106	0, 1, 34, 3, 37, 11, 15, 16, 17, 43, 24, 57, 26, 27, 30	Intermediate
107	0, 3, 5, 10, 12, 14, 21, 25, 28, 31, 32, 33, 38, 43, 44, 45, 46, 50, 57, 58, 63, 64	Intermediate
108	4, 5, 6, 7, 9, 10, 12, 17, 18, 20, 21, 26, 28, 34, 35, 36, 38, 43, 44, 48, 54, 55, 56, 58, 59, 60, 63	Intermediate
109	3, 5, 10, 12, 15, 16, 18, 26, 28, 35, 41, 43, 44, 45, 46, 47, 50, 52, 57, 58, 59, 60, 63, 64	Intermediate
110	4, 40, 10, 52, 54, 59, 63	Intermediate
111	0, 1, 2, 3, 4, 5, 7, 10	Intermediate
112	0, 1, 3, 4, 5, 6, 7, 9, 10, 17, 19, 20, 21, 23, 26, 34, 36, 38, 43, 44, 46, 48, 54, 55, 56, 58, 59, 63	Intermediate
113	0, 1, 3	Intermediate
114	0, 1, 3, 12, 13, 14, 18, 19, 21, 22, 23, 25, 28, 29, 31, 32, 33, 35, 36, 37, 38, 39, 45, 46, 51, 53, 56, 58, 60, 61, 62, 64	Intermediate
115	0, 1, 2, 3, 5, 7, 46, 19, 23	Intermediate
116	1, 2, 3, 4, 5, 7, 10, 11, 13, 15, 16, 17, 18, 19, 22, 23, 24, 26, 27, 29, 30, 34, 35, 36, 37, 39, 43, 45, 46, 51, 53, 56, 57, 58, 64	Intermediate
117	2, 4, 37, 6, 7, 9, 10, 61, 48, 49, 55, 60, 42, 62, 5	Intermediate
118	0, 1, 2, 3, 5, 7	Intermediate
119	0, 1, 3, 40, 52, 54, 59, 60, 61, 62, 63	Intermediate
120	0, 32, 34, 43, 38, 33, 11, 12, 14, 15, 16, 17, 21, 25, 24, 57, 26, 27, 28, 30, 31	Intermediate
121	34, 4, 37, 38, 7, 63, 10, 43, 44, 48, 17, 20, 21, 54, 55, 56, 36, 26, 59, 58, 5	Intermediate
122	0, 1, 3, 4, 8, 10, 13, 18, 19, 22, 23, 29, 35, 39, 40, 41, 45, 46, 47, 50, 52, 54, 59, 63	Intermediate
123	0, 1, 2, 3, 4, 5, 6, 7, 9, 10, 48, 49, 55, 42	Intermediate
124	0, 1, 3, 8, 44, 46, 50, 19, 20, 23	Intermediate
125	48, 59, 4, 6, 41, 10, 55, 47, 16, 49, 52, 9, 26, 15, 42	Intermediate
126	0, 1, 2, 3, 4, 5, 7, 10	Intermediate
127	1, 2, 3, 5, 6, 7, 9, 13, 18, 19, 22, 23, 29, 35, 36, 37, 39, 42, 45, 46, 48, 49, 51, 53, 55, 56, 58, 64	Intermediate
128	0, 32, 38, 33, 12, 14, 21, 25, 28, 31	Intermediate
129	1, 3, 6, 9, 13, 15, 16, 18, 19, 22, 23, 26, 29, 35, 36, 37, 39, 41, 42, 45, 46, 47, 48, 49, 51, 52, 53, 55, 56, 58, 59, 64	Intermediate
130	28, 18, 35, 12, 60	Intermediate
131	2, 43, 5, 6, 7, 9, 11, 34, 15, 16, 17, 24, 57, 26, 27, 30	Intermediate
133	0, 1, 2, 3, 4, 5, 7, 10	Intermediate
134	0, 6, 8, 9, 12, 13, 14, 18, 19, 21, 22, 23, 25, 28, 29, 31, 32, 33, 35, 38, 39, 40, 41, 45, 46, 47, 50, 52, 54, 59, 63	Intermediate
135	32, 2, 35, 5, 7, 60, 39, 12, 45, 14, 47, 49, 18, 22, 9, 28, 62	Intermediate
136	3, 5, 6, 9, 10, 15, 16, 26, 37, 41, 43, 44, 45, 46, 47, 50, 52, 57, 58, 59, 63, 64	Intermediate
137	4, 5, 7, 9, 10, 14, 17, 19, 20, 21, 22, 23, 26, 32, 34, 36, 38, 39, 43, 44, 45, 46, 47, 48, 49, 54, 55, 56, 58, 59, 62, 63	Intermediate
138	1, 3, 11, 13, 15, 16, 17, 18, 19, 22, 23, 24, 26, 27, 29, 30, 34, 35, 36, 37, 39, 43, 45, 46, 51, 53, 56, 57, 58, 64	Intermediate
140	0, 1, 2, 3, 4, 5, 6, 7, 9, 10, 15, 27, 30, 31, 33, 37, 42, 48, 49, 51, 53, 55, 57, 61, 64	Intermediate
141	0, 1, 2, 3, 5, 6, 7, 9, 60, 61, 62	Intermediate
142	0, 32, 38, 33, 12, 14, 21, 25, 28, 31	Intermediate
143	0, 1, 2, 6, 8, 11, 12, 13, 15, 16, 18, 19, 23, 24, 25, 27, 28, 29, 30, 31, 33, 35, 37, 40, 41, 42, 51, 52, 53	Intermediate
144	0, 6, 8, 9, 11, 12, 13, 14, 15, 16, 17, 18, 19, 21, 22, 23, 24, 25, 26, 27, 28, 29, 30, 31, 32, 33, 34, 35, 38, 39, 41, 43, 45, 46, 47, 50, 57	Intermediate
145	2, 43, 5, 7, 11, 34, 46, 15, 16, 17, 19, 23, 24, 57, 26, 27, 30	Intermediate
146	0, 1, 3, 4, 6, 60, 10, 55, 12, 48, 49, 18, 35, 9, 28, 42	Intermediate
147	0, 32, 59, 37, 38, 33, 31, 41, 12, 46, 47, 16, 19, 52, 14, 23, 25, 26, 15, 28, 21	Intermediate
148	0, 1, 3	Intermediate
149	37	Intermediate
150	1, 3, 11, 13, 15, 16, 17, 18, 19, 22, 23, 24, 26, 27, 29, 30, 34, 35, 36, 37, 39, 43, 45, 46, 51, 53, 56, 57, 58, 64	Intermediate
151	2, 5, 7, 8, 44, 50, 20	Intermediate
152	0, 1, 34, 3, 11, 15, 16, 17, 43, 24, 57, 26, 27, 30	N.D.
153	0, 1, 3, 4, 5, 8, 10, 11, 13, 14, 17, 20, 21, 22, 24, 25, 29, 32, 34, 36, 38, 39, 40, 43, 44, 45, 46, 50, 54, 56, 57, 58, 63, 64	N.D.
154	0, 1, 2, 3, 4, 5, 6, 7, 9, 10, 60, 61, 62	N.D.
155	0, 6, 9, 11, 12, 14, 15, 16, 17, 21, 24, 25, 26, 27, 28, 30, 31, 32, 33, 34, 38, 42, 43, 48, 49, 55, 57	N.D.
157	0, 1, 2, 4, 5, 6, 7, 8, 9, 11, 13, 14, 15, 16, 17, 20, 21, 22, 24, 25, 26, 29, 32, 34, 36, 37, 38, 39, 40, 41, 42, 47, 48, 49, 52, 54, 55, 56, 59	Poor
158	9, 10, 4, 6	Poor
159	0, 1, 4, 8, 11, 13, 14, 17, 20, 21, 22, 24, 25, 29, 32, 34, 36, 38, 39, 40, 54, 56, 60, 61, 62	Poor
160	0, 1, 4, 8, 11, 13, 14, 17, 20, 21, 22, 24, 25, 29, 32, 34, 36, 38, 39, 40, 54, 56	Poor
161	10, 4	Poor
162	0, 1, 3, 4, 37, 10	Poor
163	32, 39, 9, 45, 14, 47, 49, 22, 62	Poor
164	9, 11, 12, 14, 15, 16, 17, 18, 22, 24, 26, 27, 28, 30, 32, 34, 35, 37, 39, 40, 43, 45, 47, 49, 52, 54, 57, 59, 60, 62, 63	Poor
165	37	Poor
166	0, 1, 4, 6, 8, 9, 11, 13, 14, 17, 20, 21, 22, 24, 25, 29, 32, 34, 36, 38, 39, 40, 54, 56	Poor
167	19, 46, 23	Poor
168	59, 37, 6, 41, 47, 16, 52, 9, 26, 15	Poor
169	9, 6	Poor
170	0, 1, 4, 8, 11, 13, 14, 15, 17, 20, 21, 22, 24, 25, 27, 29, 30, 31, 32, 33, 34, 36, 37, 38, 39, 40, 51, 53, 54, 56, 57, 61, 64	Poor
171	60, 37, 62, 61	Poor
172	10, 4	Poor
174	46, 19, 23, 60, 61, 62	Poor
175	0, 1, 4, 8, 11, 13, 14, 17, 19, 20, 21, 22, 23, 24, 25, 29, 32, 34, 36, 38, 39, 40, 46, 54, 56	Poor
176	0, 1, 4, 6, 8, 9, 11, 13, 14, 15, 17, 20, 21, 22, 24, 25, 27, 29, 30, 31, 32, 33, 34, 36, 37, 38, 39, 40, 51, 53, 54, 56, 57, 61, 64	Poor
177	2, 5, 7, 8, 44, 46, 50, 19, 20, 23	Poor
178	4, 6, 40, 9, 10, 61, 48, 49, 52, 54, 55, 59, 60, 42, 62, 63	Poor
179	2, 5, 7, 9, 11, 14, 15, 16, 17, 22, 24, 26, 27, 30, 32, 34, 39, 43, 45, 47, 49, 57, 62	Poor
180	2, 59, 4, 5, 7, 8, 41, 10, 44, 15, 16, 50, 52, 20, 26, 47	Poor

181	60, 61, 62	Poor
183	4, 5, 7, 10, 17, 20, 21, 26, 34, 36, 37, 38, 43, 44, 48, 54, 55, 56, 58, 59, 60, 61, 62, 63	Poor
184	0, 1, 2, 3, 4, 5, 7, 8, 10, 19, 20, 24, 25, 27, 28, 29, 31, 32, 34, 35, 38, 39, 42, 44, 49, 50, 51, 55, 56	Poor
186	0, 1, 4, 6, 8, 9, 11, 13, 14, 17, 20, 21, 22, 24, 25, 29, 32, 34, 36, 38, 39, 40, 54, 56	Poor
187	0, 32, 2, 6, 5, 38, 7, 8, 12, 44, 14, 50, 20, 21, 9, 25, 33, 28, 31	Poor
188	32, 51, 34, 35, 6, 38, 39, 9, 42, 49, 19, 56, 55, 24, 25, 27, 28, 29, 31	Poor
189	0, 1, 4, 8, 11, 13, 14, 17, 20, 21, 22, 24, 25, 29, 32, 34, 36, 38, 39, 40, 54, 56	Poor
190	0, 1, 3, 4, 5, 8, 10, 11, 13, 14, 17, 20, 21, 22, 24, 25, 29, 32, 34, 36, 38, 39, 40, 43, 44, 45, 46, 50, 54, 56, 57, 58, 63, 64	Poor
191	0, 1, 4, 8, 11, 12, 13, 14, 17, 18, 19, 20, 21, 22, 23, 24, 25, 28, 29, 32, 34, 35, 36, 38, 39, 40, 46, 54, 56, 60	Poor
192	4, 5, 7, 8, 10, 13, 15, 17, 18, 19, 20, 21, 22, 23, 26, 27, 29, 30, 31, 33, 34, 35, 36, 37, 38, 39, 41, 43, 44, 45, 46, 47, 48, 50, 51, 53, 54,55, 56, 57, 58, 59, 61, 63, 64	Poor
194	0, 1, 4, 6, 8, 9, 11, 13, 14, 17, 20, 21, 22, 24, 25, 29, 32, 34, 36, 38, 39, 40, 54, 56	Poor
195	0, 1, 4, 8, 11, 13, 14, 17, 20, 21, 22, 24, 25, 29, 32, 34, 36, 38, 39, 40, 54, 56	Poor
196	0, 1, 2, 3, 5, 6, 7, 9, 46, 19, 23, 60, 61, 62	Poor
197	2, 35, 5, 6, 7, 8, 12, 44, 18, 60, 50, 20, 9, 28	Poor
198	0, 1, 4, 8, 11, 13, 14, 17, 20, 21, 22, 24, 25, 29, 32, 34, 36, 37, 38, 39, 40, 54, 56	Poor
199	8, 44, 50, 20	Poor